successBRT

RTsafe

SBRT Remote End-to-End Dosimetry Auditing Service Report

@ Hospital

Report reviewed by: Evangelos Pappas,
Associate Professor of Medical Physics,
University of West Attica
Medical Physics Expert, MPE

Audit outcome: PASS

Audit Date: J DDth Month YYYY

RTsafe is an ISO certified company:

APPROVAL SWISS CERT ISO 9001

APPROVAL SWISS CERT ISO 13485

successSBRT

RTsafe
48, Artotinis str
116 33, Athens
Greece
+30 2107563691
info@rt-safe.com

Institution:	Hospital
Date of audit:	Month DD YYYY
Date of report:	Month DD YYYY
Institution's contact person:	Name
Report reviewed by:	Evangelos Pappas Associate Professor of Medical Physics
Phantom:	SBRT phantom
Treatment planning system:	TPS
Treatment delivery modality:	LINAC/ CK / GK
Treatment delivery unit:	Model
Image Guidance/setup/positioning protocol:	CBCT
Phantom S/N:	1219SBRT
Film Insert Kit S/N:	3620FDK
OSLD Insert Kit S/N:	0220OSLDK
Gel Insert Kit S/N (empty-gel / filled):	-- / --

Contents

Introduction

RTsafe's succesS^{B}RT audit is a remote end-to-end dosimetry audit service for stereotactic body radiotherapy (SBRT) applications. The primary objective of succesS^{B}RT audit is to evaluate the dosimetric quality, planned dose accuracy and treatment deliverability of body SRT procedures for the improvement of standards and reliability of the institutions.

The scope of this report is to:

- Present and assess the dosimetric impact of all steps of the SBRT treatment pathway through an end-to-end test, i.e., immobilization, pre-treatment imaging, treatment planning, setup - image guidance and dose delivery, and
- Outline the quality of the delivered treatment in the radiotherapy center based on point and 2D dosimetry results, as recorded and reviewed from the dosimetry audit.

The phantom used in the audit was the RTsafe SBRT phantom, using the specially designed inserts to accommodate Gafchromic EBT films and optically stimulated luminescent (OSL) dosimeters (Figure 1). All the dosimeters are calibrated at the Secondary Standard Dosimetry Laboratory of the Greek Atomic Energy Commission, providing traceability to BIPM-France. The users received an RT structure set with the target and the critical structures and were challenged to achieve a specific level of accuracy for the required treatment objectives.

Figure 1: The RTsafe SBRT phantom, along with the appropriate inserts to accommodate Gafchromic EBT film and OSL dosimeters.

Audit Procedures

Preparation for the audit

The Hospital received the SBRT phantom (RTsafe P.C.) on on Month DDth YYYY. SBRT was accompanied with the corresponding inserts for film and OSL dosimeters. For absolute OSL dosimetry, the corresponding insert was pre-loaded with 17 calibrated OSLDs (Figure 2c), allowing measurements in the coronal plane. Similarly, for absolute 2D dosimetry, two (2) calibrated pre-cut EBT-3 films were available for measurements in the sagittal and coronal planes (Figure 2a, 2b).

The phantom was prepared for CT scanning for a liver stereotactic body radiotherapy treatment. Then three consecutive CT scans were performed, one for each detector, with the film (coronal and sagittal orientations) and OSL detectors in place.

A separate/reference dataset of the benchmark case (CT scan of the phantom with the target and organs at risk (OAR) volumes) was provided in DICOM format via the RTsafe secure sharing platform. All CT scans were imported into the Treatment Planning System (TPS). The target (PTV = 33.8 cc), located within the liver and close to the right kidney and the bowel, was delineated such that its center of mass lies at the film plane.

All CT scans of the phantom were co-registered in the TPS. The delineated contours were propagated to the local CT scans onto which the dose calculations were performed. Figure 2 shows a schematic of the location of the OSL and film dosimetry cassettes, relative to the PTV and OARs.

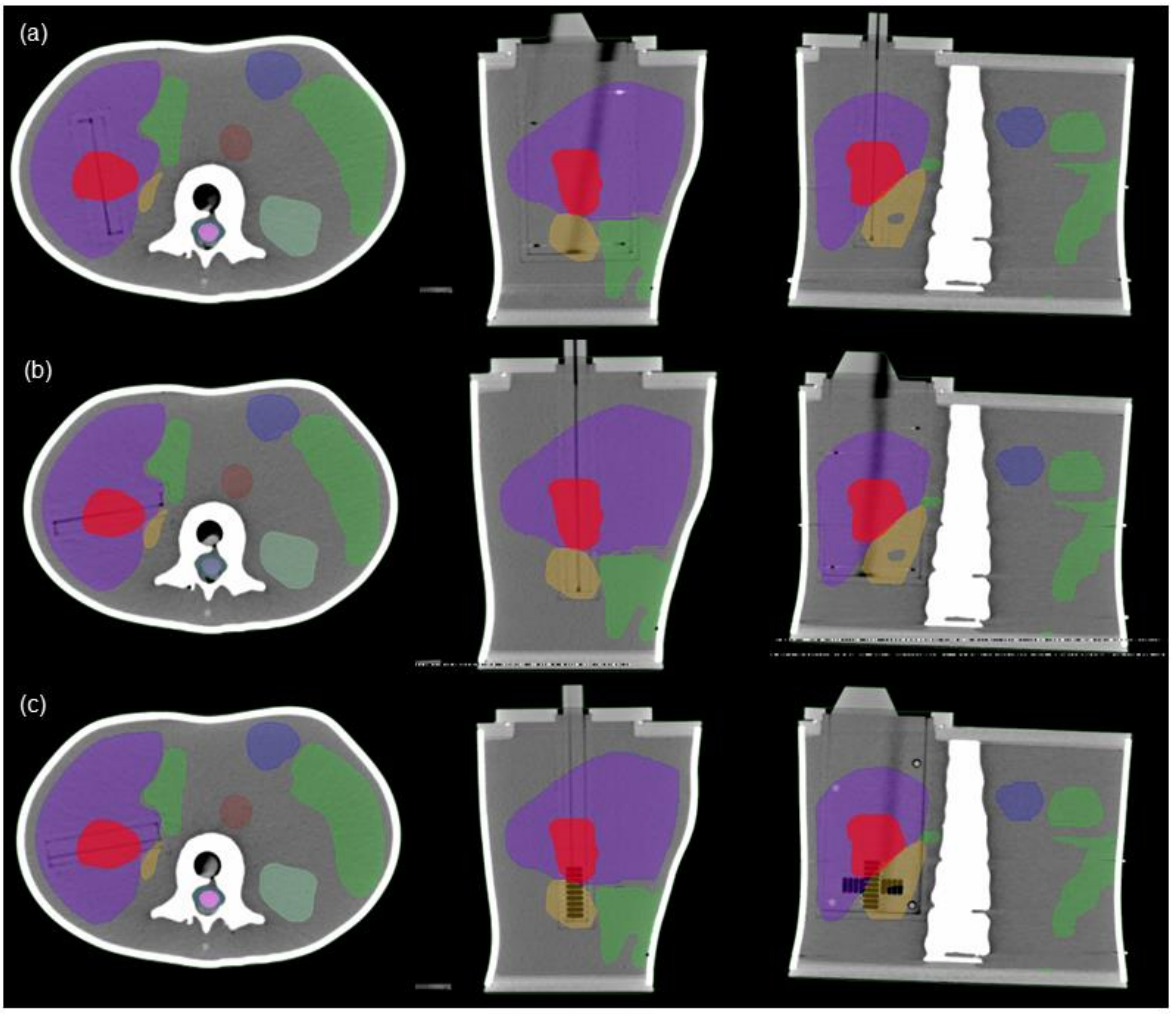

Figure 2: Schematic representation of the axial, sagittal and coronal planes through the phantom showing (a)-(b) film and (c) OSL dosimeters.

The SBRT treatment plan was generated following the local protocol by the staff members who normally perform the patient treatment planning and exported to the treatment delivery platform. The treatment objectives that the user was asked to achieve during the planning process are shown in Table 1. A treatment plan was generated using the TPS. The DICOM RT plan, dose, and structure set files were sent back to RTsafe via the RTsafe secure sharing platform.

Table 1: Treatment optimization objectives & dose goals.

Structure:		
PTV	95% of volume to receive at least 45 Gy	5 fractions
Quality metrics:		
Max dose within PTV	60 Gy	
Normal Liver	Mean dose of normal liver (liver – GTV) less than 10 Gy	
Kidney_R	Less than 50% of the volume of the right kidney to receive 5 Gy (V5Gy < 50%)	
Bowel	Less than 0.035 cc of the volume of bowel to receive 15Gy < 0.035cc	

SBRT plan delivery

The end-to-end procedure was performed by the RT center staff according to the local protocol.

Two different dosimetry inserts were used; the film and OSL dosimetry cassettes. Thus, the institution subsequently irradiated three (3) times the SBRT phantom (two (2) for film irradiations in sagittal and coronal orientations and one (1) for the OSLDs irradiation in coronal plane).

Plan data was sent to the linear accelerator for delivery. The SBRT phantom incorporating the film dosimeters were treated first. The process was repeated for the OSL measurements.

After completion, the SBRT phantom and the dosimetry inserts were returned to RTsafe and OSL and film dosimeters were unloaded for analysis.

The end-to-end dosimetric and geometric accuracy were evaluated. Absolute (OSLDs & films) agreement with TPS calculations was assessed in terms of 1D dose profiles and 1D gamma index, 2D isolines and 2D gamma index maps and 3D gamma index passing rates for the target.

Auditors' assessments

SBRT plan evaluation

The submitted treatment plan parameters are shown in Table 2.

Table 2: Treatment plan parameters.

Treatment plan name:	
Technique:	
Treatment delivery modality:	
Treatment delivery unit:	
TPS:	
Dose calculation algorithm:	--
Energy:	7FFF
Total treatment time / Total Monitor Units (Mus):	--
Dose prescription (Gy):	45
Number of fractions:	5
Dose per fraction (Gy):	9
Dose grid resolution exported (x, y, z):	1 mm x 1 mm x 1 mm
Maximum Dose (Gy):	57.63
CT scan in plane resolution (mm):	0.7826x0.7826
CT scan slice thickness (mm):	1

OSL dosimetry

Point-dose comparison

OSLD results are given in Table 3. Wherever applicable, appropriate correction factors have been applied to the OSLD response in order to take into account the individual sensitivity of each dosimeter, $k_{s,i}$, potential signal fading and depletion effects, dose-response nonlinearity and orientation dependency, according to the recommendations of AAPM TG-191[1].

To facilitate the reader to understand the results, Figure 3 shows the position of the dosimeters on the cassette.

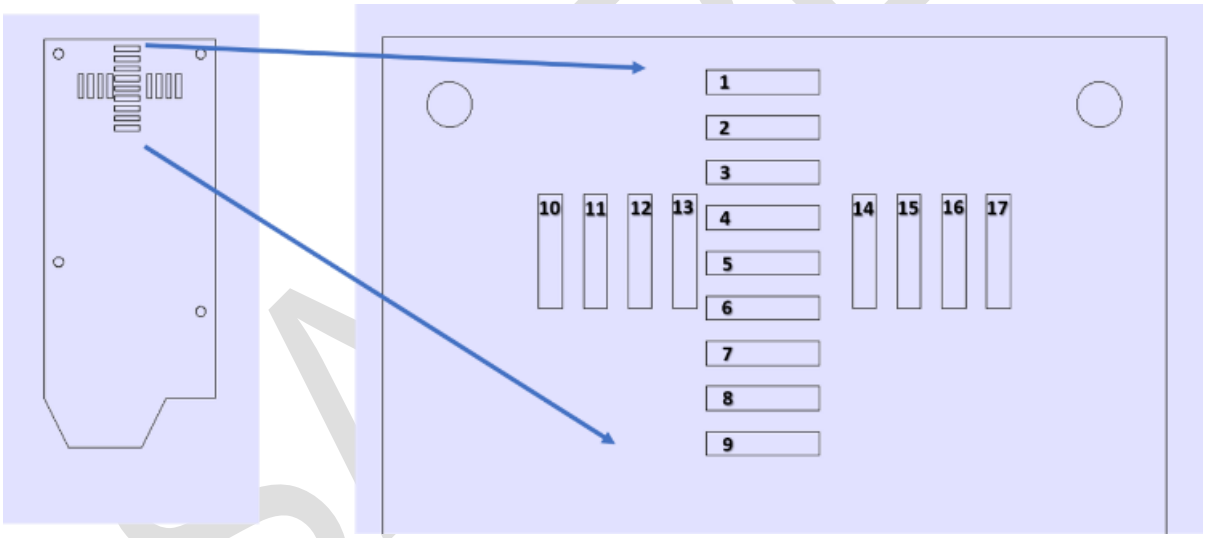

Figure 3: Schematic representation of the dosimetry cassette placed along the coronal plane through the phantom showing all OSL dosimeters.

Table 3: OSL dosimetry results of the end-to-end procedures using the Prime phantom. The total combined uncertainty at k=1 is ± 3%. Position IDs are defined in Figure 3.

Position IDs	TPS calculated dose per fraction (Gy)	OSL measured dose (Gy)	Dose difference (%)	GI 5%/1.5mm Global	GI 3%/2mm Local
1	10.54	10.84	2.78	0.559	0.733
2	10.45	10.31	-1.38	0.298	0.349
3	10.55	10.74	1.80	0.388	0.444
4	10.59	10.64	0.40	0.090	0.099
5	10.32	10.41	0.86	0.182	0.203
6	10.32	10.24	-0.71	0.114	0.096
7	10.59	10.25	-3.38	0.684	0.850
8	9.81	9.60	-2.11	0.205	0.162
9	7.11	7.36	3.34	0.168	0.149
10	9.43	9.40	-0.29	0.062	0.058
11	9.60	9.59	-0.12	0.017	0.027
12	9.90	10.40	4.82	0.854	**1.093**
13	10.15	10.13	-0.20	0.044	0.060
14	10.22	10.09	-1.29	0.265	0.344
15	10.09	9.95	-1.38	0.273	0.308
16	9.67	9.68	0.05	0.019	0.029
17	9.22	9.10	-1.30	0.211	0.218
			Fails #:	0	1
			Passing rate:	100.00%	94.10%

Lateral (right-left) and superior-inferior absolute dose profiles for the OSL-measured and TPS-calculated datasets for PTV 1 are presented in Figures 4 & 5, respectively. Error bars correspond to ± 5% dosimetric and ± 1.5 mm spatial uncertainty.

Gamma index calculations were also performed in 3D and results are included in Figures 4 & 5. A selection of gamma passing criteria, suitable for SBRT plan analysis, were considered.

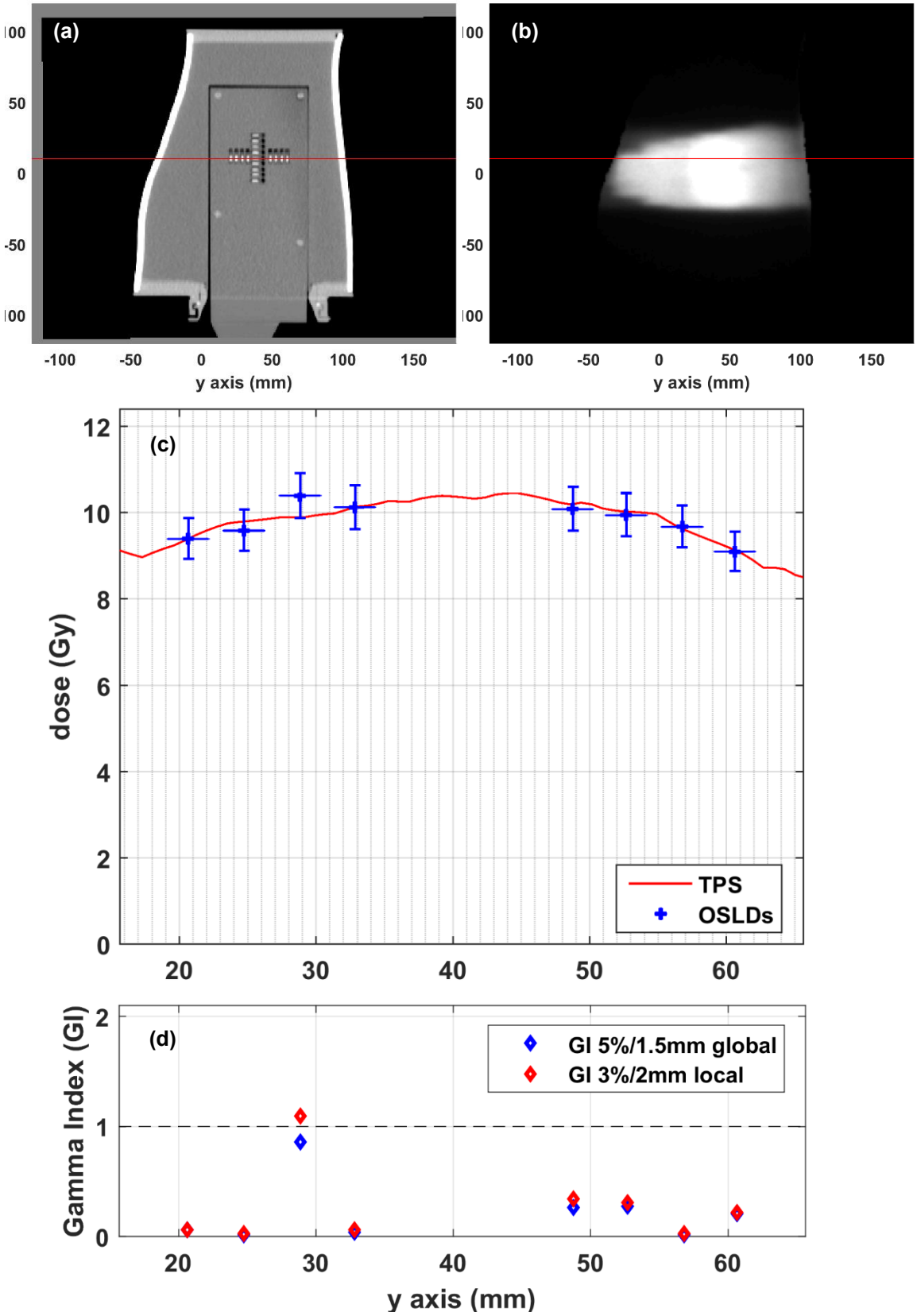

Figure 4: Lateral dose profile for PTV 1 - (a) A central slice of the CT image stack of the phantom incorporating the OSLDs and (b) the corresponding slice of the TPS-calculated dose distribution (exported in the RTDOSE file). The red solid line displays the direction in which the OSLDs active volumes lie. (c) 1D profile comparison between calculated (TPS) and measured (OSL) datasets at the dosimeters locations according to the direction depicted by the red solid line. (d) 3D gamma index calculations are also given, considering the following passing criteria: global 5%/1.5mm & local 3%/2mm.

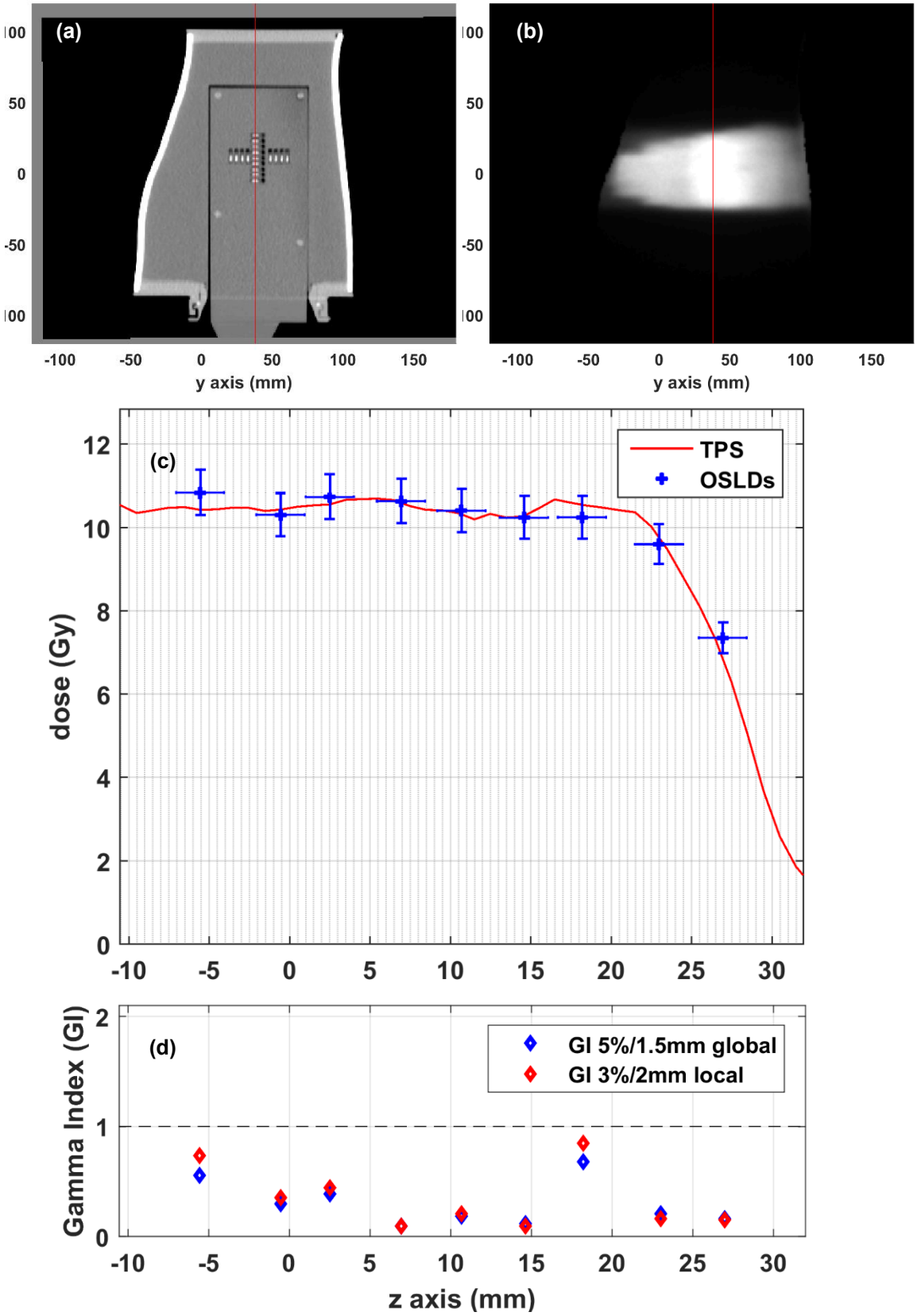

Figure 5: Superior-inferior dose profile for PTV 1 - (a) A central slice of the CT image stack of the phantom incorporating the OSLDs and (b) the corresponding slice of the TPS-calculated dose distribution (exported in the RTDOSE file). The red solid line displays the direction in which the OSLDs active volumes lie. (c) 1D profile comparison between calculated (TPS) and measured (OSL) datasets at the dosimeters locations according to the direction depicted by the red solid line. (d) 3D gamma index calculations are also given, considering the following passing criteria: global 5%/1.5mm & local 3%/2mm.

Film dosimetry

Profile's comparison

A right-left and a superior-inferior absolute dose profiles for the film-measured and TPS-calculated datasets are presented in the following figures 6-11 for all targets.

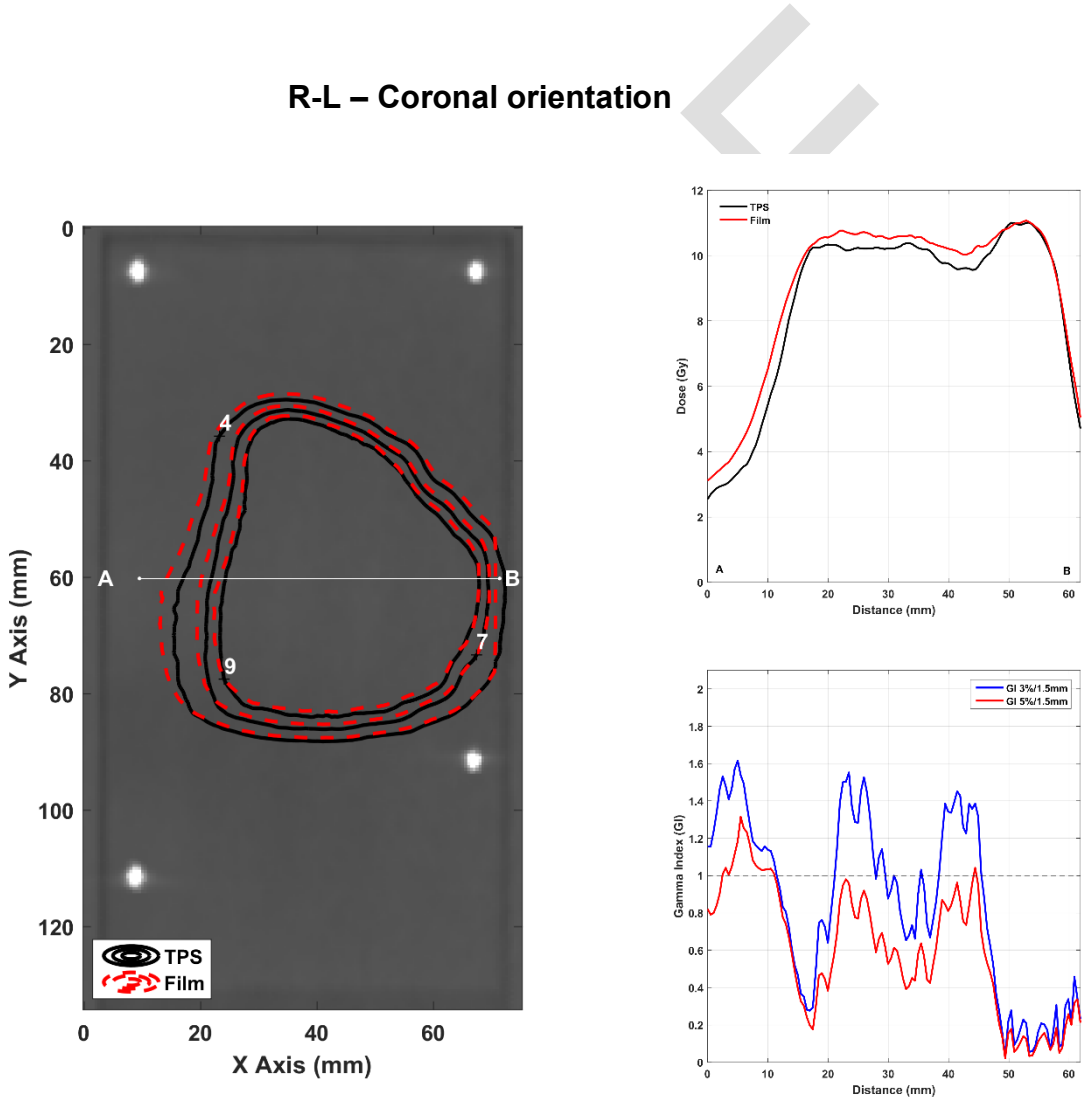

Figure 6: PTV - (left) Slice of the reconstructed CT scan of the film phantom. Contours correspond to TPS calculations (black solid lines) and film measurements (red dashed lines) in Gy. (right) 1D profile comparison between calculated (TPS) and measured (Film) dose distributions at the location depicted by the white line. 1D gamma index calculations are also given using passing criteria 3%/1.5mm & 5%/1.5mm.

Sup-Inf – Coronal orientation

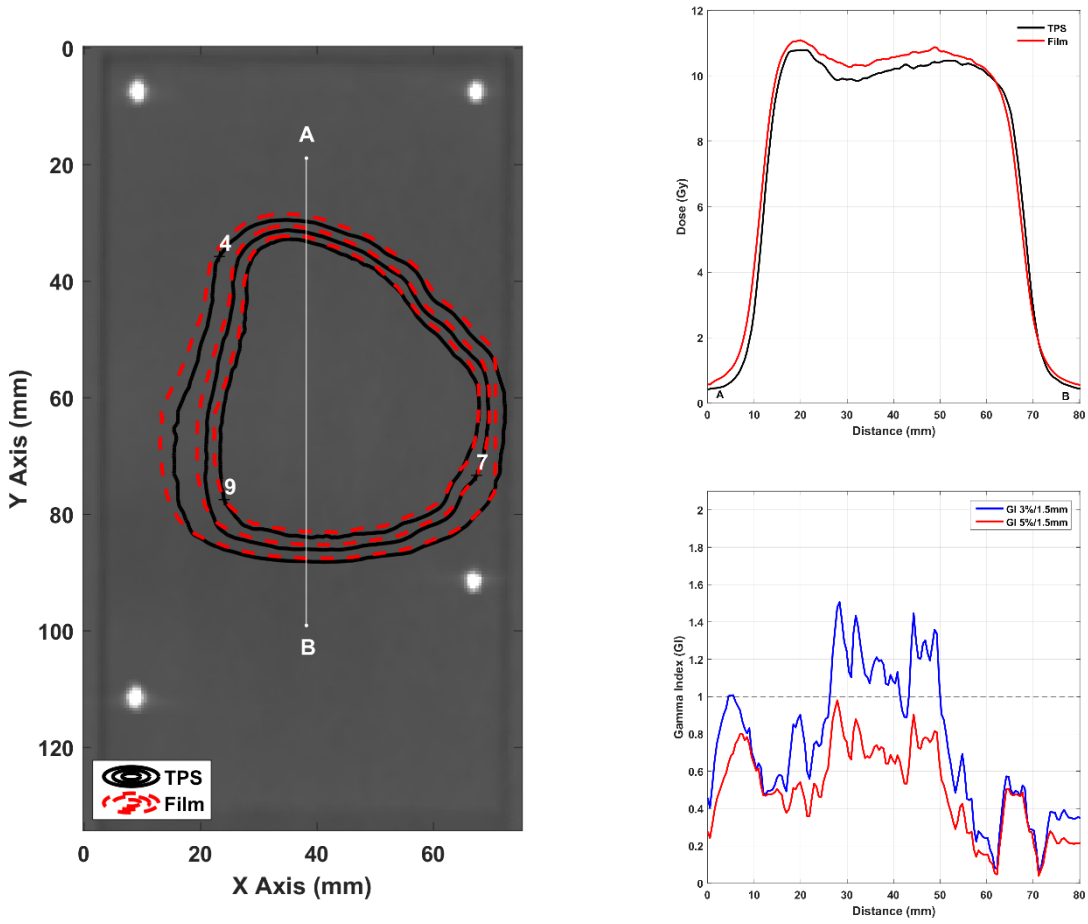

Figure 7: PTV - (left) Slice of the reconstructed CT scan of the film phantom. Contours correspond to TPS calculations (black solid lines) and film measurements (red dashed lines) in Gy. (right) 1D profile comparison between calculated (TPS) and measured (Film) dose distributions at the location depicted by the white line. 1D gamma index calculations are also given using passing criteria 3%/1.5mm & 5%/1.5mm.

A-P – Sagittal orientation

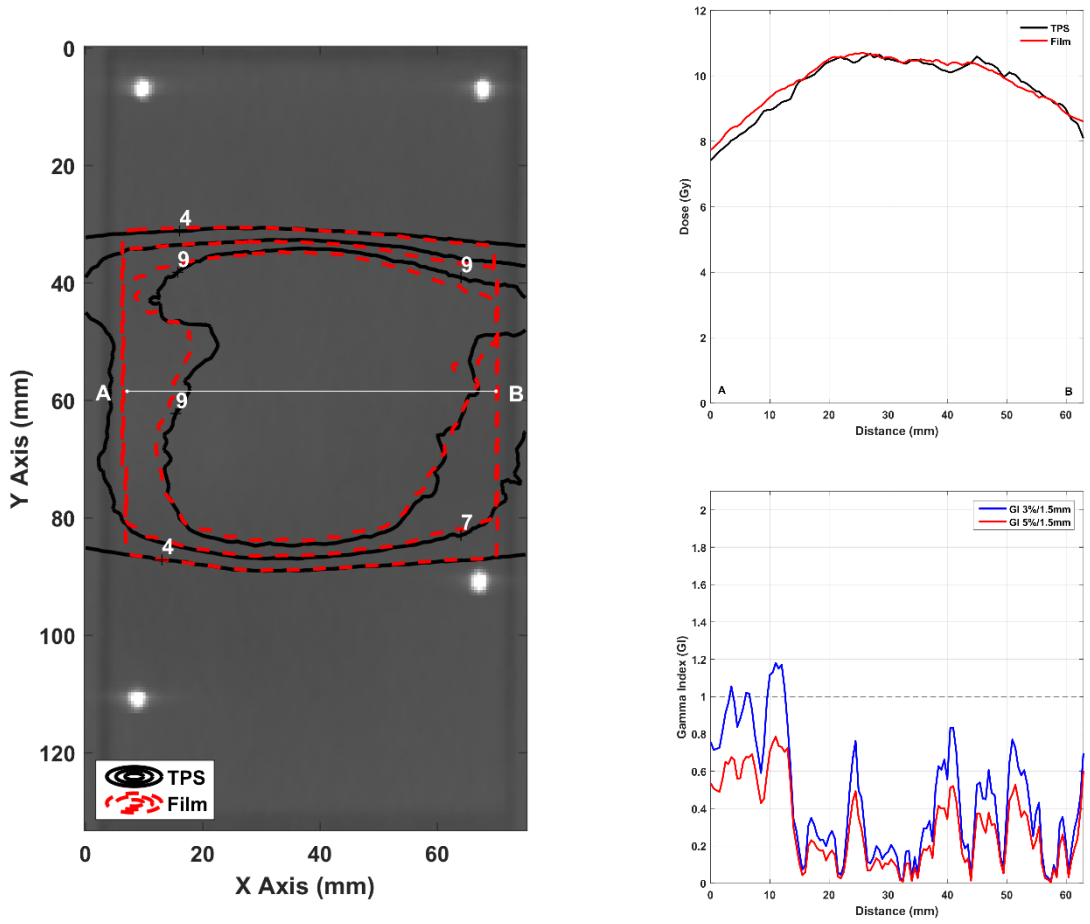

Figure 8: PTV - (left) Slice of the reconstructed CT scan of the film phantom. Contours correspond to TPS calculations (black solid lines) and film measurements (red dashed lines) in Gy. (right) 1D profile comparison between calculated (TPS) and measured (Film) dose distributions at the location depicted by the white line. 1D gamma index calculations are also given using passing criteria 3%/1.5mm & 5%/1.5mm.

Sup-Inf – Sagittal orientation

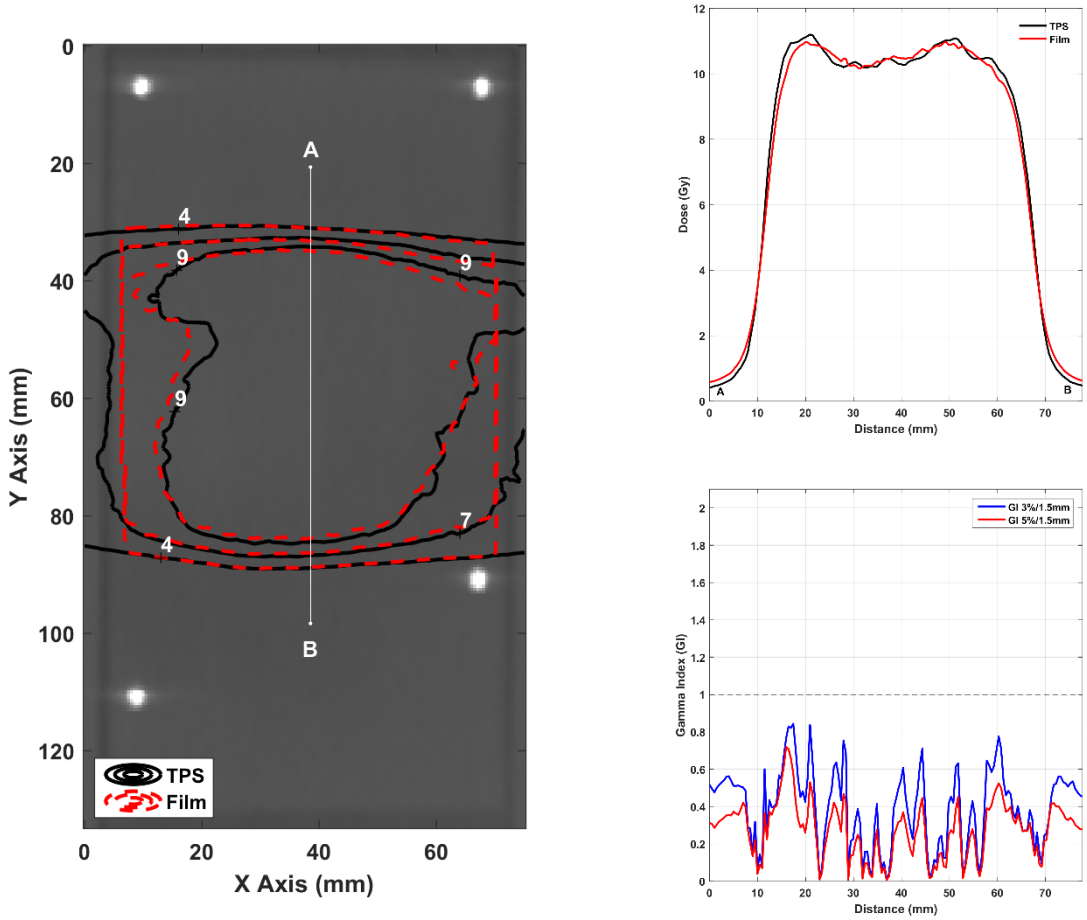

Figure 9: PTV - (left) Slice of the reconstructed CT scan of the film phantom. Contours correspond to TPS calculations (black solid lines) and film measurements (red dashed lines) in Gy. (right) 1D profile comparison between calculated (TPS) and measured (Film) dose distributions at the location depicted by the white line. 1D gamma index calculations are also given using passing criteria 3%/1.5mm & 5%/1.5mm.

2D Gamma Index comparison

For the slice between film cassette slabs of the film phantom, 3D gamma index calculations (i.e., reference data: 2D film measurements, evaluated data: 3D TPS calculations) are presented in the following figures. Passing criteria for global gamma index calculations were 5%/1.5mm and 3%/1.5mm and for local gamma index calculations 3%/2mm dose difference and distance-to-agreement, respectively. A low-dose cut-off threshold of 20% of the maximum dose has been applied to exclude corresponding voxels from the gamma index calculations. Isodose lines are also plotted to assist comparison.

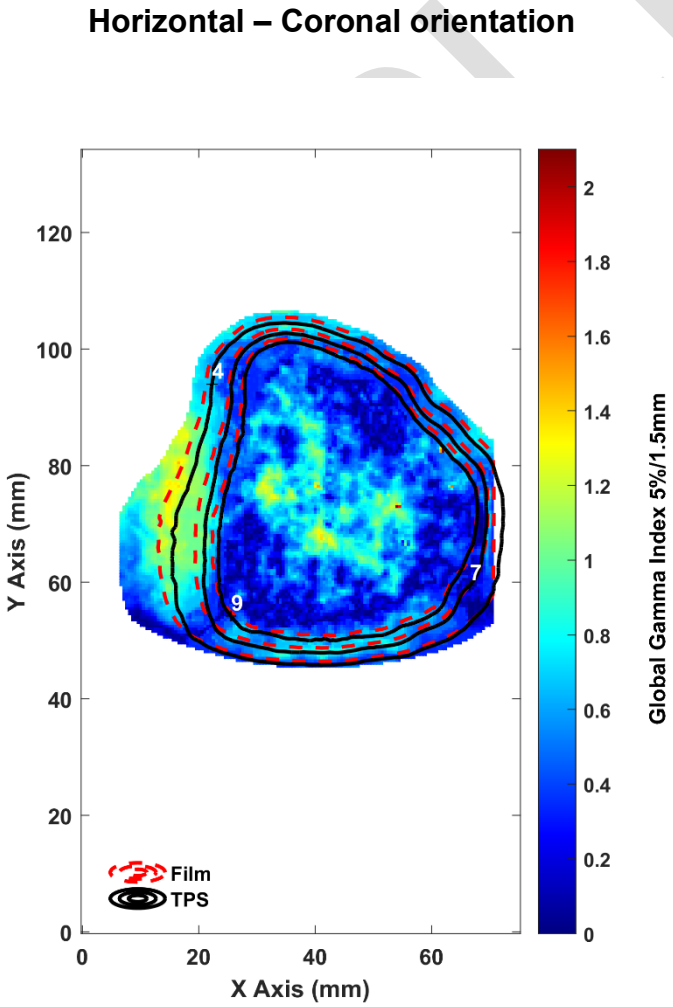

Figure 12: 2D comparison between calculated (TPS) and measured (Film) dose distributions in Gy values applying a 20% low-dose cut-off threshold. 3D global gamma index calculations are given using passing criteria 5%/1.5mm.

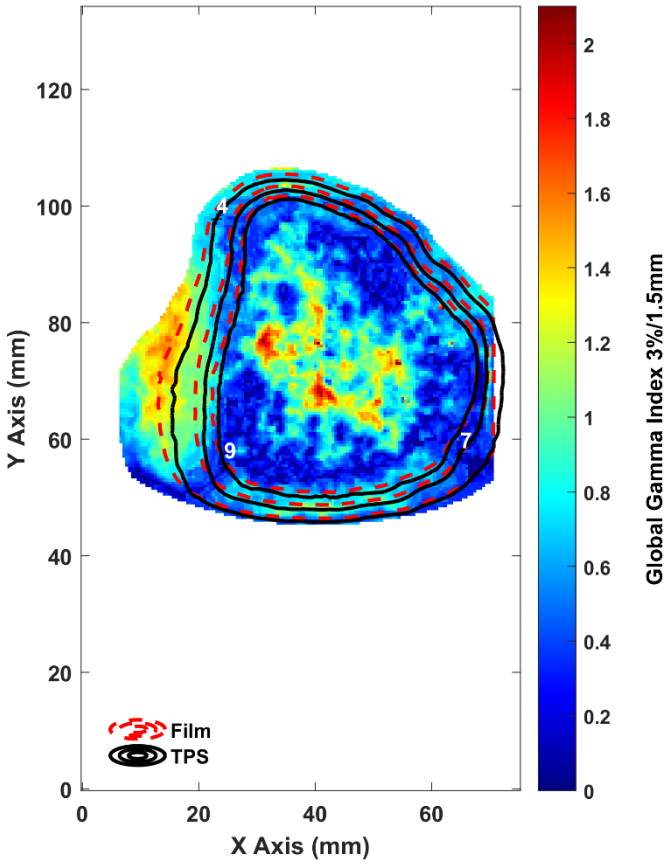

Figure 13: 2D comparison between calculated (TPS) and measured (Film) dose distributions in Gy values applying a 20% low-dose cut-off threshold. 3D global gamma index calculations are given using passing criteria 3%/1.5mm.

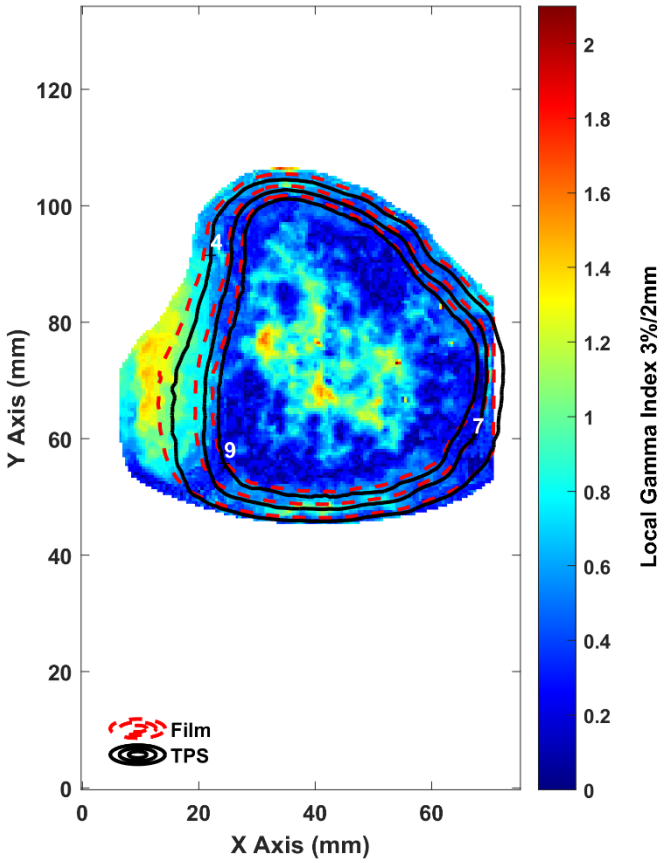

Figure 14: 2D comparison between calculated (TPS) and measured (Film) dose distributions in Gy values applying a 20% low-dose cut-off threshold. 3D local gamma index calculations are given using passing criteria 3%/2mm.

Vertical – Sagittal orientation

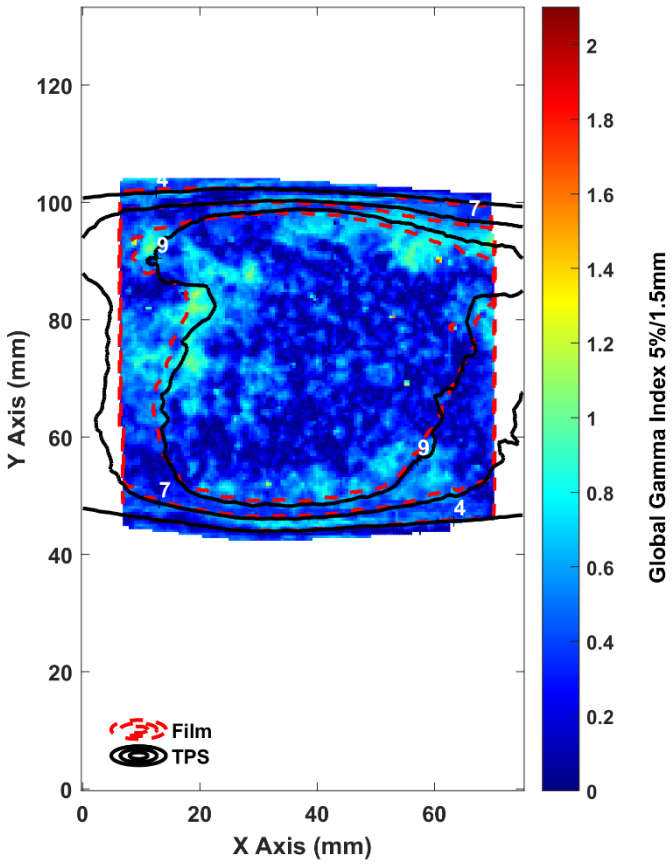

Figure 15: 2D comparison between calculated (TPS) and measured (Film) dose distributions in Gy values applying a 20% low-dose cut-off threshold. 3D global gamma index calculations are given using passing criteria 5%/1.5mm.

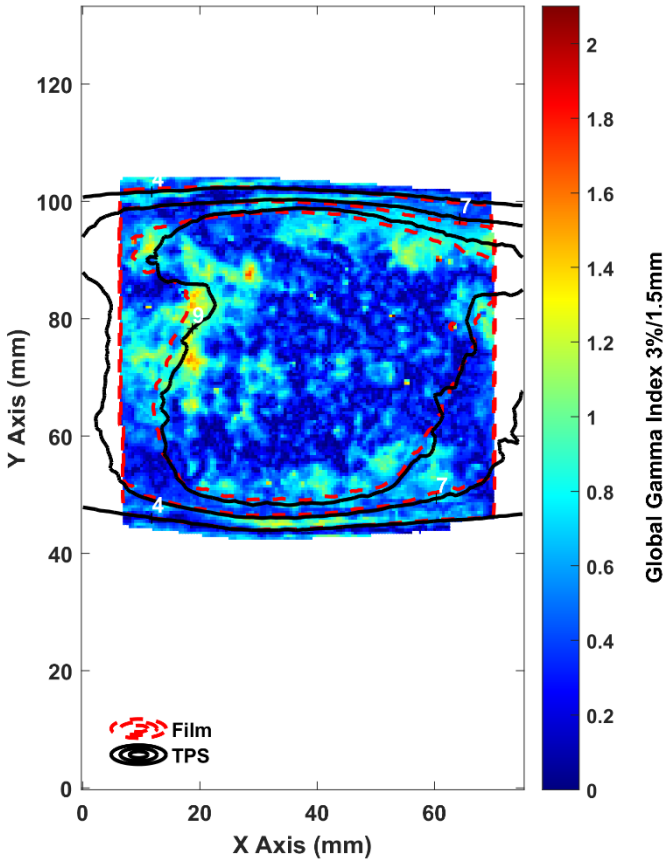

Figure 16: 2D comparison between calculated (TPS) and measured (Film) dose distributions in Gy values applying a 20% low-dose cut-off threshold. 3D global gamma index calculations are given using passing criteria 3%/1.5mm.

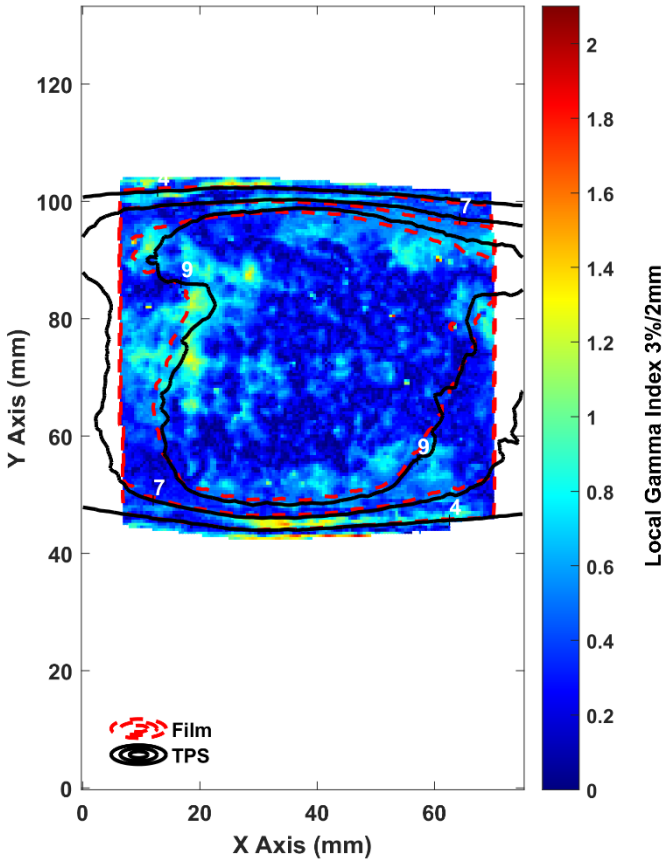

Figure 17: 2D comparison between calculated (TPS) and measured (Film) dose distributions in Gy values applying a 20% low-dose cut-off threshold. 3D local gamma index calculations are given using passing criteria 3%/2mm.

3D Gamma Index comparison

Gamma index calculations were also performed in 3D. A selection of gamma passing rates suitable for SBRT plan analysis were chosen. The gamma passing rates presented were collected using the red color channel covering the area of the film, with a low-dose cut-off threshold of 20% of the maximum dose. Corresponding results are summarized in the following tables (4 & 5).

Table 4: Results for the 3D gamma index test of Film 1 in coronal orientation (Horizontal), comparing film-measured (reference) with the TPS-calculated (evaluated) dose distributions using a variety of passing criteria. Note that passing rates were calculated using a low-dose cut-off threshold of 20% of the maximum dose.

Structure	Passing criteria			GI Passing Rate
	DD (%)	DTA (mm)		GI ≤ 1 (%)
Film Plane	3	3	global	98.46
	3	2	global	90.37
	3	1.5	global	80.79
	2	2	global	84.46
	5	**1.5**	**global**	**91.82**
	3	2	local	90.00

Table 5: Results for the 3D gamma index test of Film 2 in sagittal orientation (Vertical), comparing film-measured (reference) with the TPS-calculated (evaluated) dose distributions using a variety of passing criteria. Note that passing rates were calculated using a low-dose cut-off threshold of 20% of the maximum dose.

Structure	Passing criteria			GI Passing Rate
	DD (%)	DTA (mm)		GI ≤ 1 (%)
Film Plane	3	3	global	99.92
	3	2	global	98.94
	3	1.5	global	96.20
	2	2	global	97.26
	5	**1.5**	**global**	**99.58**
	3	2	local	97.86

To quantify the overall performance and adequacy of the dosimetric commissioning, the tolerance limits, proposed by AAPM-RSS Medical Physics Practice Guideline 9.a. for SRS-SBRT were adopted. In detail, using IGRT system, the E2E localization assessment should be ≤ 1 mm and the E2E dosimetric evaluation should lie within ± 5% difference of the measured versus the calculated dose distributions. Therefore, for the gamma analyses, the tolerance limit is set to ≥ 95%, with 5%/1.5 mm and a 20% low-dose cut-off threshold and the action limit to ≥ 90%, with 5%/1.5 mm and a 20% low-dose cut-off threshold, having a gamma <1.

Audit outcome

The analysis performed has not indicated any concerns regarding the local practices for the specific aspects of dosimetry for stereotactic body radiotherapy. All dose computations during treatment planning (calculation algorithm, medium corrections, dose reporting) are in compliance with RTOG protocol requirements. As it was beyond the objectives of this study, critical organ dose-volume data are not presented, however, organ-at-risk doses were constrained in accordance with RTOG protocol guidelines. Dosimetry results meet the listed acceptance criteria proposed by AAPM-RSS Medical Physics Practice Guideline 9.a. for SRS-SBRT.

APPENDIX. Dosimeter's readout and analysis process

OSL dosimetry

The phantom incorporating the OSLD dosimetry case is similar to the detailed description in the publication of Makris et al 20191. The difference is that instead of the film cassette, the OSLD cassette of the same dimensions is in-place. The cassette may accommodate up to 17 OSLDs in a cross-shape distribution, lying centrally on the upper side of the cassette plane (Figure 4a). The myOSLchip OSL dosimeters (RadPro, https://www.radpro-int.com/osl/) were employed for end-to-end absolute point dosimetry in the RTsafe Prime phantom. Their sensitive (active) volume is made of beryllium oxide (BeO) with dimensions of 4.65 x 4.65 x 0.5 mm^3. For dose-readout of the irradiated OSLDs, the myOSLchip mobile reader was used.

Dose determination using OSLDs was performed by following the relevant recommendations of the "High Accuracy" protocol described in AAPM TG-191 report2. Briefly, this report defines and suggests a set of correction factors to be determined and applied wherever applicable in a dosimetry procedure.

The individual sensitivity factor, $k_{s,i}$ was determined for each OSLD of the same batch. This correction factor is used to account for the variations of the sensitivity between each dosimeter in the same batch. $k_{s,i}$ represents the ratio of an individual dosimeter's response to a predefined uniform dose (M_i) to the mean response to the same dose from all the detectors in the batch ($\bar{M}$).

$k_{s,i} = \bar{M} / M_i$ (1).

For the determination of the $k_{s,i}$ correction factor, a conventional 6MV linear accelerator with a flattened 10x10 cm² field and a TPR20,10 of 0.676 was used. A uniform dose of 50 cGy was delivered to all OSLDs comprising this batch, and each detector was read three times. In this context, M_i in Equation 1 is calculated as the average raw signal from the three readouts.

Furthermore, dose-response nonlinearity of the batch was characterized by irradiating OSLDs (in groups of nine) to uniform dose levels, up to 14Gy, using the reference 10 x 10 cm^2 field. Appropriate linearity correction factors, k_L, were determined and applied, if relevant. In a similar approach, orientation and fading correction factors, k_θ and k_f, respectively, were also determined and applied if relevant.

Sensitivity of the dosimetric system is assessed within the context of the calibration coefficient, $N_{D,w}$. This quantity represents the sensitivity of the batch in combination with the reader and the readout parameters for a given set of irradiation conditions, in Gy/counts. It can be determined by irradiating standards at a predefined dose using the reference 10 x 10 cm^2 field. This irradiation is performed on the same day as the dosimetry audit test and readout is carried out on the same reading session. This approach ensures similar irradiation and readout conditions between the standards and the experimentals (e.g., same photon beam energy, fading, photomultiplier sensitivity, batch sensitivity drifting, etc.).

17 detectors were used in this dosimetry procedure, and another 9 from the same batch served as standards for session-specific $N_{D,w}$ determination, according to the definitions and protocol of AAPM TG-191. Each detector, i, was readout and the raw signal, $M_{raw,i}$, was corrected using the corresponding $k_{s,i}$ and after subtracting the background signal determined following OSLD bleaching:

$M_{corr,i} = k_{s,i} * (M_{raw,i} - \text{Bkg})$ (2).

The absorbed dose to water Dw, by the clinical beam quality, Q, is determined by:

$$D_w = M_{corr} \cdot N_{D,w} \cdot k_F \cdot k_L \cdot k_Q \cdot k_\theta \quad (3)$$

where M_{corr} is the corrected OSLD signal, according to Equation (2). Correction factors in Eq (3) are applied to account for the differences in irradiation and readout conditions between the standard (for $N_{D,w}$ determination) and the experimental (used for the audit test). Given that beam quality and fading was matched, k_Q and k_F are unity by definition.

To determine the corresponding TPS dose points to be compared with the measurement results the OSLDs sensitive volumes were contoured in the TPS and the mean dose of each sensitive volume was considered as a point dose at the coordinates od the center of each OSLD's sensitive volume.

For the SBRT plan, the dose difference between TPS predicted and OSLD measured doses in the sensitive volume of each dosimeter was calculated and reported as:

$$\frac{D^{TPS} - D^{OSLD}}{D^{OSLD}} \; x \; 100\%$$

The typical uncertainty budget for the OSLD dosimetry protocol is given in Table 1. The Type A and Type B columns include the relative standard uncertainties (percentage, for k=1).

Table 1: Uncertainty analysis for the OSL dose measurements using Prime phantom.

	Spatial, mm	**Type A, %**	**Type B, %**
Calibration factors			
Reference irradiation accuracy / Linac output	N/A	-	1.5
Calibration coefficient, $N_{D,w,}$ (variation of standards)	N/A	1.1	-
Reader factors			
Readout accuracy	N/A	-	1.0
Readout reproducibility	N/A	0.6	-
Detector factors			
Individual sensitivity factor, $k_{s,i}$	N/A	0.6	-
Linearity correction factor, k_L	N/A	-	1.0
Angular correction factor, k_θ	N/A	-	1.3
Active volume localization in the CT image stack	0.5	N/A	N/A
Total standard uncertainties	0.5	1.4	2.4
Combined total standard uncertainty, k=1	**0.5**	**2.8**	
Expanded uncertainty, k=2	**1.0**	**5.6**	

Film dosimetry

The phantom incorporating the film dosimetry cassette, has been described in detail in the publication of Makris et al 2019[2]. The EBT-3 Gafchromic films were employed for end-to-end absolute 2D dosimetry in the RTsafe Prime phantom. Each film piece was handled according to the procedures summarized in Niroomand-Rad et al[6]. The films were scanned on an EPSON V850 Pro flatbed color scanner in transmission mode, with maximum optical density (OD) range and all filters and image enhancement options disabled. All films (calibration and experimental) were labeled and scanned in landscape orientation with respect to the scanning bed, pre- and 24h post-irradiation. RGB positive images are collected at 48-bit RGB with a spatial resolution of 150 dpi (0.169 mm pixel size) and saved as tagged image file format (TIFF) files.

The dose calibration of the film batch was performed in the IRCL/GAEC-EIM at a Co-60 beam. Film pieces of dimensions 4×4 cm^2 were irradiated at a depth of 5 cm in a Solid Water HE slab phantom (Sun Nuclear Corporation) for doses ranging from of 0.10 to 15 Gy.

Each film piece was scanned five times. The obtained images are processed using a custom-made software tool (Graphical User Interface, GUI) developed in MATLAB (MathWorks, Natick, MA). The red, green and blue components of the RGB image are separated. The net Optical Density, netOD, was determined for the red color channel[7]. A polynomial calibration curve was obtained for the red color and was used for conversion of the net optical density values into dose values[8]. Experimental dose maps were also calculated using the single channel method proposed by Devic[8–10].

One film piece 7.5 x 14 cm^2 of the EBT-3 film was placed in the appropriate dosimetry cassette of the Prime phantom. The cassette contains 4 metal pins in order to facilitate film positioning and spatial registration of the film dose distribution with the exported RTDOSE from the treatment planning system (TPS). The geometric center of the fiducials is located on the film plane. Matching the CT-identified centers of the fiducials with corresponding positions of the holes in the scanned film image offers the necessary set of reference

points, defining the rigid transformation matrix in order to spatially register film measurements to TPS calculations.

The typical uncertainty budget for the film calibration, which includes film irradiation and scanner factors, is presented in the following Table 4. The Type A and Type B columns include the relative standard uncertainties (percentage, for k=1).

The film dose distribution is compared to the corresponding slice of the RTDOSE, exported from the RT center's TPS in a uniform 0.5 mm resolution grid.

The typical uncertainty budget for the film dose distribution measurement, which includes irradiation and film and scanner factors, is presented in the following table 5. The Type A and Type B columns include the relative standard uncertainties (percentage, for k=1).

To assess whether the QA results meet the pre-defined standards the latest recommendations of the AAPM-RSS Medical Physics Practice Guideline 9.a. for SRS-SBRT[11] are adopted. So, following these recommendations for gamma analysis using global normalization in absolute dose tolerance limits are set as follows:

• Tolerance limits: the γ passing rate should be ≥ 95%, with 5%/1 mm and a 10% low-dose cut-off threshold.

• Action limits: the γ passing rate should be ≥ 90%, with 5%/1 mm and a 10% low-dose cut-off threshold.

Table 3: Uncertainty analysis for the dose distribution measurement on the film during the end-to-end procedures using Prime phantom.

	Spatial, mm	Type A, %	Type B, %	
Calibration factors				
Reference irradiation accuracy	N/A		0.55	
Phantom positioning during irradiation (*)	N/A		0.20	
Solid water to water dose correction (*)	N/A	0.50		
			Dose dependent	
Calibration curve fit parameters (dose dependent)	N/A		2.16	3.17
Scanner factors				
Reproducibility (*)	N/A	0.15		
OD measurement reproducibility	N/A	0.40		
Scanner homogeneity (*)	N/A		0.20	
Registration factors				
OSL plane and positioning (CT, TPS and LINAC)	0.5	N/A	N/A	
Combined Type A and Type B standard uncertainties	0.5	0.66	2.25	3.23
Combined standard uncertainty, k=1	**0.5**	**2.34**	**3.30**	
Expanded uncertainty, k=2	N/A	**4.69**	**6.59**	

(*)[3,12,13]

References

1. Kry SF, Alvarez P, Cygler JE, et al. AAPM TG 191: Clinical use of luminescent dosimeters: TLDs and OSLDs. *Med Phys*. 2020;47(2):e19-e51. doi:10.1002/mp.13839
2. Makris DN, Pappas EP, Zoros E, et al. Characterization of a novel 3D printed patient specific phantom for quality assurance in cranial stereotactic radiosurgery applications. *Phys Med Biol*. 2019;64(10). doi:10.1088/1361-6560/ab1758
3. Wesolowska PE, Cole A, Santos T, Bokulic T, Kazantsev P, Izewska J. Characterization of three solid state dosimetry systems for use in high energy photon dosimetry audits in radiotherapy. *Radiat Meas*. 2017;106:556-562. doi:10.1016/j.radmeas.2017.04.017
4. Viamonte A, Da Rosa LAR, Buckley LA, Cherpak A, Cygler JE. Radiotherapy dosimetry using a commercial OSL system. *Med Phys*. 2008;35(4):1261-1266. doi:10.1118/1.2841940
5. Yukihara EG, Yoshimura EM, Lindstrom TD, Ahmad S, Taylor KK, Mardirossian G. High-precision dosimetry for radiotherapy using the optically stimulated luminescence technique and thin Al2O3:C dosimeters. *Phys Med Biol*. 2005;50(23):5619-5628. doi:10.1088/0031-9155/50/23/014
6. Niroomand-Rad A, Chiu-Tsao ST, Grams MP, et al. Report of AAPM Task Group 235 Radiochromic Film Dosimetry: An Update to TG-55. *Med Phys*. 2020;47(12):5986-6025. doi:10.1002/mp.14497
7. Méndez I. Model selection for radiochromic film dosimetry. *Phys Med Biol*. 2015;60:4089-4104.
8. Devic S, Seuntjens J, Sham E, et al. Precise radiochromic film dosimetry using a flat-bed document scanner. *Med Phys*. 2005;32(7Part1):2245-2253. doi:10.1118/1.1929253
9. Devic S, Tomic N, Lewis D. Reference radiochromic film dosimetry: Review of technical aspects. *Phys Medica*. 2016;32(4):541-556. doi:10.1016/j.ejmp.2016.02.008
10. Devic S, Seuntjens J, Hegyi G, et al. Dosimetric properties of improved GafChromic films for seven different digitizers. *Med Phys*. 2004;31(9):2392-2401. doi:10.1118/1.1776691
11. Halvorsen PH, Cirino E, Das IJ, et al. AAPM-RSS Medical Physics Practice Guideline 9.a. for SRS-SBRT. *J Appl Clin Med Phys*. 2017;18(5):10-21. doi:10.1002/acm2.12146
12. Mathot M, Sobczak S, Hoornaert MT. Gafchromic film dosimetry: Four years experience using FilmQA Pro software and Epson flatbed scanners. *Phys Medica*. 2014;30(8):871-877. doi:10.1016/j.ejmp.2014.06.043
13. Aldelaijan S, Mohammed H, Tomic N, et al. Radiochromic film dosimetry of HDR 192Ir source radiation fields. *Med Phys*. 2011;38(11):6074-6083. doi:10.1118/1.3651482
14. Daniel Saenz, Niko Papanikolaou, Emmanouil Zoros, Evangelos Pappas, Michael Reiner, Lip Teck Chew, Hooi Yin Lim, Sam Hancock, Alex Nebelsky, Christopher Njeh GA. Robustness of single-isocenter multiple-metastasis stereotactic radiosurgery end-to-end testing across institutions. *J Radiosurg SBRT*. 2021;7(3):223-232. Accessed May 24, 2021. https://pubmed.ncbi.nlm.nih.gov/33898086/
15. Hillbrand M, Landry G, Ebert S, et al. Gel dosimetry for three dimensional proton range measurements in anthropomorphic geometries. *Z Med Phys*. 2019;29(2):162-172. doi:10.1016/j.zemedi.2018.08.002
16. Saenz DL, Li Y, Rasmussen K, Stathakis S, Pappas E, Papanikolaou N. Dosimetric and localization accuracy of Elekta high definition dynamic radiosurgery. *Phys Medica*. 2018;54(August):146-151. doi:10.1016/j.ejmp.2018.10.003
17. Pappas E, Maris T, Angelopoulos A, et al. A new polymer gel for magnetic resonance imaging (MRI) radiation dosimetry. *Phys Med Biol*. 1999;44(10):2677-2684. doi:10.1088/0031-9155/44/10/320
18. Pantelis E, Moutsatsos A, Antypas C, et al. On the total system error of a robotic radiosurgery system: Phantom measurements, clinical evaluation and long-term analysis. *Phys Med Biol*. 2018;63(16). doi:10.1088/1361-6560/aad516
19. Moutsatsos A, Karaiskos P, Petrokokkinos L, et al. On the use of polymer gels for assessing the total geometrical accuracy in clinical Gamma Knife radiosurgery applications. *J Phys Conf Ser*. 2010;250:292-296. doi:10.1088/1742-6596/250/1/012060

RTsafe is an ISO certified company: